In situ lift-off InAs quantum dots by pulsed laser irradiation

Changwei Deng,[1,2,a)] Zhenwu Shi,[1,2,b)] Linyun Yang,[1,2,a)] Wei Zhang,[3] Chen Chen,[1,2] Lili Miao,[1,2] Xinning Yang,[1,2] Chinhua Wang,[1,2] Linsen Chen,[1] and Changsi Peng[1,2,4,b)]

[1]*School of Optoelectronic Science and Engineering & Collaborative Innovation Center of Suzhou Nano Science and Technology, Soochow University, Suzhou 215006, China.*

[2]*Key Lab of Advanced Optical Manufacturing Technologies of Jiangsu Province & Key Lab of Modern Optical Technologies of Education Ministry of China, Soochow University, Suzhou 215006, China.*

[3]*Suzhou Institute of Nano-Tech and Nano-Bionics, Chinese Academy of Sciences, Suzhou 215123, China.*

[4]*Institute for Research in Applicable Computing, University of Bedfordshire, Park Square, Luton LU1 3JU, UK.*

InAs/GaAs quantum dots (QDs) grown by molecular beam epitaxy were subjected to in situ irradiation using a mono-beam pulsed laser. The evolution of the QD morphology was investigated as a function of irradiation intensity at temperatures of 525 °C and 480 °C. The temperature was found to exert a considerable influence on the reaction of the QDs to the irradiation. At the higher temperature (525 °C), both the height and width of the InAs QDs gradually decreased with increasing irradiation intensity, which was ascribed to the dominant effect of the laser desorption of indium. In contrast, at the lower temperature (480 °C), the height of the InAs islands decreased with increasing irradiation intensity while the width exhibited unexpected broadening, which was attributed to a combination of laser desorption and laser diffusion of indium. Remarkably, at the higher temperature, laser irradiation above a certain threshold

a) Co-first authors: These authors contributed equally to this work.

b) Electronic mail: zwshi@suda.edu.cn (Z. Shi), changsipeng@suda.edu.cn (C. Peng).

29

30 intensity resulted in the lift off of the InAs QDs to afford a clear, smooth, and perfect
31 GaAs surface. Through subsequent growth of QDs on this surface, it was found that the
32 QDs exhibited the same nucleation properties and optical quality as the common
33 Stranski–Krastanov mode on an as-prepared GaAs surface. Therefore, we have
34 developed a technology for the damage-resistant fabrication of QDs using in situ pulsed
35 laser irradiation, which is expected to find potential applications in the manufacture of
36 patterned QDs upon upgrading the mono-beam irradiation to multi-beam interference
37 irradiation in the future.

38

39 Due to 3-dimentional carrier comfinement,[1] semiconductor quantum dots (QDs)
40 are used to realize a tremendous variety of applications ranging from electronic devices
41 to photonic devices.[2,3] The Stranski–Krastanov (SK) growth mode is typically used to
42 prepare semiconductor QDs with the advantages of low defect formation, simplicity,
43 and maturity.[4] One prototypical case is the SK growth of InAs/GaAs QDs by molecular
44 beam epitaxy (MBE), and its related devices such as photodetectors,[5,6] lasers,[7,8] LEDs,[9]
45 solar cells,[10] etc.,[11,12] have been extensively fabricated. However, the cutting-edge
46 applications based on QDs, such as single-photon emitters,[13,14] quantum computation,[15]
47 and photonic crystals[16] require more controllability during QD fabrication, especially
48 with respect to site control. Since SK growth is a thermodynamic process, QD
49 nucleation occurs randomly. This drawback has substantially limited the use of normal
50 SK growth, and massive research attention has thus been devoted to pursuing new
51 methods for achieving an ordered QD arrangement. For example, it has been reported
52 that the growth of multiple layers of QDs can improve the QD arrangement by strain
53 correlation,[17–19] but this arrangement is relatively too poor in the control precision and
54 moreover, such bottom multilayers are an undesirable parasitic structure for device
55 applications. At present, self-assembling QDs on a pre-patterned substrate**Error!**

56 **Reference source not found.** is widely acknowledged as the most scalable and feasible
57 approach for ordered QD growth. However, there are still several shortcomings greatly
58 challenged the technology of patterned substrate: (a) Oxidation, pollution, and crystal
59 damage of the substrate inevitably occur during the patterning process; (b) It is very
60 hard to achieve devices with two or more patterned QD layers especially whose
61 interspace is quite small, because the first buried QD layer may be damaged when
62 performing the second patterning step on the interlayer.

63 In this paper, we investigated an in situ pulsed laser irradiation (LIR) of InAs QDs
64 grown on a GaAs (001) surface. It was found the LIR could targeted lift off the InAs
65 QDs from the substrate to leave a clear, smooth, and perfect GaAs surface. Therefore,
66 a potential damage-resistant fabrication of patterned QD can be easily foreseen and
67 realized by upgrading the mono-beam irradiation to multi-beam interference irradiation
68 that could solve all of the aforementioned problems of the patterned substrate approach.
69 First, pollution and oxidation are directly eliminated in the in-situ process and
70 meanwhile it is also proven non-destructive. Second, if the strain correlation between
71 the QD multilayers,[18-23] is neglected, our technique can freely fabricate complex QD
72 structures via layer-by-layer stacking of the patterned QD layers in a similar manner to
73 3D printing with considerable cost and time savings.

74 The experiments were performed on a special MBE system equipped with a laser
75 viewport for performing in situ LIR. First, a 500 nm GaAs buffer layer was deposited
76 on a quarter of 2-inch deoxidized GaAs (001) substrate at 600 °C. Then, the temperature
77 was separately reduced to 525 °C (samples A) and 480 °C (sample B) for the growth of
78 InAs QDs, for which the growth rate, deposition thickness, and As flux were 0.011
79 ML/s, 1.7 ML, and 8.0×10^{-7} Torr, respectively. Then the centers of the two samples
80 were immediately followed by a mono-beam LIR with a single pulse (wavelength: 355
81 nm, duration: 10 ns, energy: 10 mJ). The entire process was monitored by reflection
82 high energy electron diffraction (RHEED). After irradiation, the surface morphology of
83 the two samples were examined by tapping-mode atomic force microscopy (AFM).
84 Because the laser spot is much smaller than the substrate, both the non-irradiated region
85 (NIRR) and irradiated region (IRR) could be examined simultaneously.

86 Figure 1(a) shows the observed morphology of the NIRR for sample A (525 °C);
87 the QD growth is just at the critical onset of nucleation with a very broad distribution
88 as shown in Figs. 1(e) and (h). Fig. 1(d) shows the morphology of the irradiated region
89 center (IRRC), where the InAs QDs have completely disappeared to afford a flat and
90 clear surface with an obvious step flow (white arrows). The RHEED revealed that the
91 LIR immediately caused the dot-like pattern to abruptly switch to a bright streak-like
92 diffraction pattern of a pure GaAs surface. This result convincingly demonstrates that
93 LIR can cleanly lift off the InAs QDs from the substrate to leave a clear, smooth, and
94 perfect GaAs surface. To further clarify the LIR, we scanned the transition between the
95 NIRR and the IRR and two representative regions (denoted IRR1 and IRR2 with
96 irradiation intensity order of "$E_{IRR1} < E_{IRR2}$") were selected for study, for which the
97 results are presented in Figs. 1(b) and (c), respectively. Figs. 1(f,g) and (i,j) show the
98 corresponding width and height distributions of the InAs QDs in IRR1 and IRR2. With
99 irradiation intensity increasing, the InAs QDs gradually decreased in both width (Figs.
100 1(e–g)) and height (Figs. 1(h–j)) and ultimately disappeared. While for sample B
101 (480 °C), four regions denoted NIRR, IRR1, IRR2, and IRRC were again selected and
102 investigated (Figs. 2(a–d)). In the IRRC (Fig. 2(d)), the InAs QDs were removed but
103 the remained surface was very rough. Thus from RHEED, the observed GaAs
104 reconstruction streaks were dispersed and not bright. In contrast to sample A, it appears
105 that the surface step flows were cracked into many irregular atomic fragments in sample
106 B (white arrows). The evolution of the InAs islands with the irradiation intensity is also
107 remarkable; as shown in Figs. 2(e–j), the height of the InAs islands gradually decreased
108 in a similar manner to sample A, but the width abnormally broadened. Consequently,
109 the substrate temperature exerts a strong influence on the effect of LIR on InAs QDs.

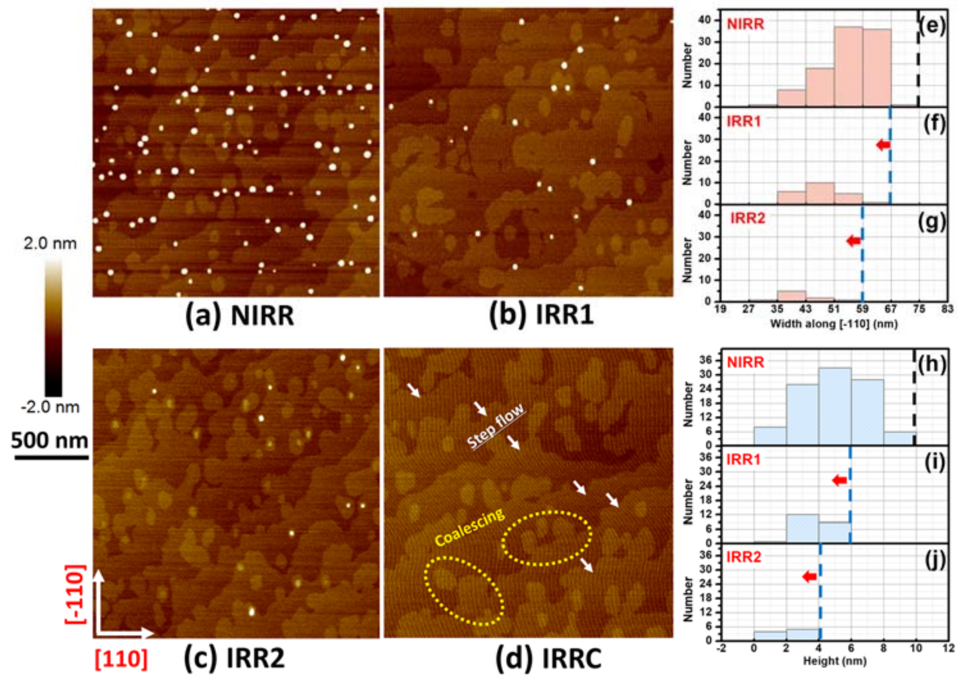

FIG. 1. (a–d) AFM morphology results in the (a) NIRR, (b) IRR1, (c) IRR2, and (d) IRRC of sample A, and (e–j) corresponding histograms of (e–g) width and (h–j) height distributions for the InAs QDs in NIRR, IRR1, and IRR2.

110

111

112

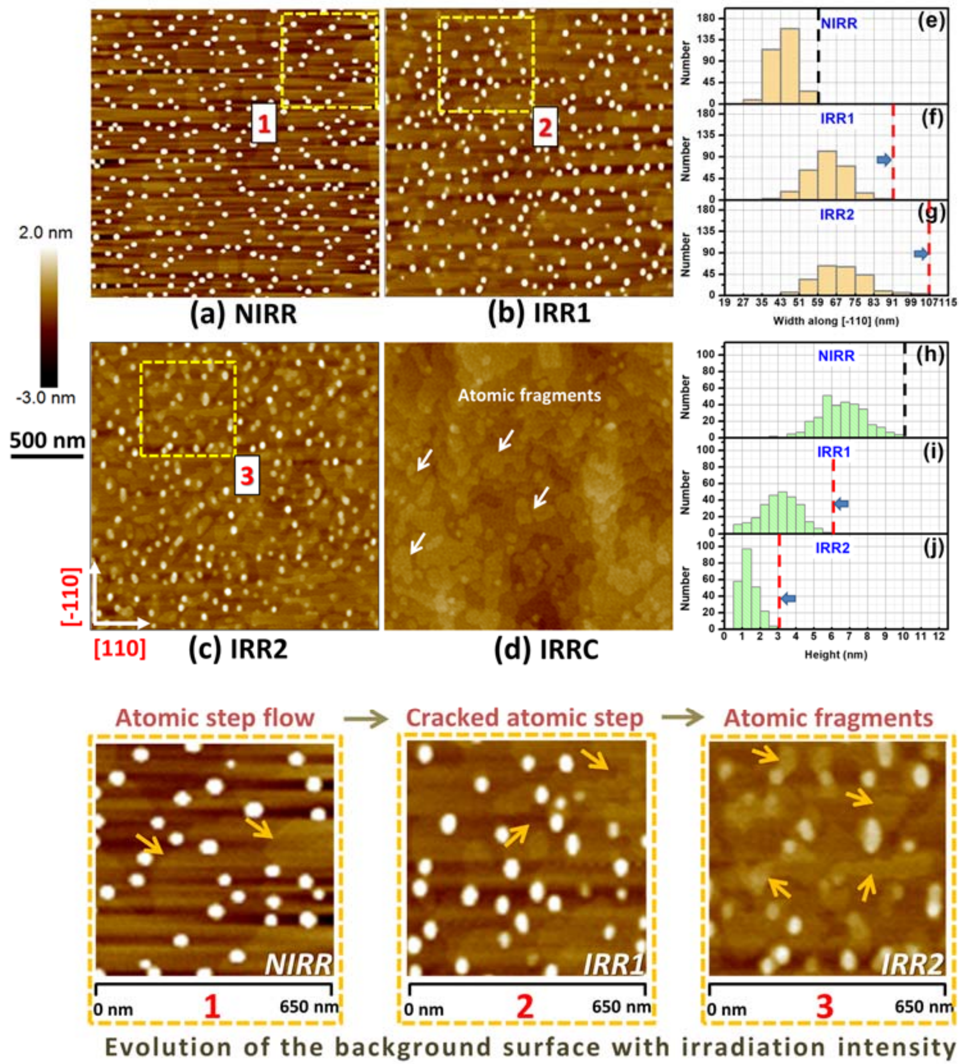

FIG. 2. (a–d) AFM morphology results in the (a) NIRR, (b) IRR1, (c) IRR2, and (d) IRRC of sample B, and (e–j) corresponding histograms of (e–g) width and (h–j) height distributions for the InAs QDs in NIRR, IRR1, and IRR2. At the bottom, three enlargements of yellow dashed squares (denoted 1–3) in (a–c) are presented.

113 To directly visualize the differences, we selected one typical island from the NIRR,
114 IRR1, and IRR2 of each sample, for which the section profiles are presented in Figs.
115 3(a) and (b). It clearly demonstrates that, for sample A, the body of the InAs QD
116 consistently maintained a "dot" shape and shrunk step-by-step during the LIR. In
117 contrast, during the LIR of sample B, the InAs QD body did not exhibit a "dot" shape
118 but deformed into 2D islands. To interpret these interesting phenomena, it should first
119 be pointed out that the InAs QDs grown at 525 °C (Fig. 1(a)) possessed a lower density
120 and smaller size than those grown at 480 °C (Fig. 2(a)), despite the identical InAs
121 deposition amount. This reflects that the adsorption coefficient of indium sharply
122 decreased at 525 °C; in other words, the indium atoms in the QDs will also become
123 extremely active and easy to evaporate. Consequently, upon LIR of sample A, the
124 indium atoms will easily be excited by the laser to overcome the vacuum barrier (Fig.
125 3(c), as indicated by the red arrow) and desorb from the surface. The laser-induced
126 desorption of indium is depicted in Fig. 3(d): the outer indium atoms would be expected
127 to desorb prior to those inside the QD body, which explains the gradual shrinkage of
128 the QDs (indicated by black arrows) with increasing irradiation intensity. Moreover, the
129 InAs QDs with a relatively small size (as observed in Fig. 1(a), a large proportion of
130 the QDs possessed a small size) would also be completely desorbed immediately after
131 irradiation thus leads to a rapid QD density reduction in IRR1 (Fig. 1(b)). Finally, the
132 clear and smooth GaAs surface observed in the IRRC (Fig. 1(d)) can be simply
133 explained by the target desorption of indium owing to the intrinsic difference in bond
134 strength between InAs and GaAs (see the vacuum barrier gap between In and Ga, as
135 depicted in Fig. 3(c)). In contrast, for sample B, the indium will become more stable at
136 480 °C and thus the desorption probability may be relatively depressed under the same
137 irradiation intensity. Consequently, some of the indium atoms will fail to desorb from
138 the surface, but they might overcome the lower diffusion barrier (the black arrow in Fig.
139 3(c)) to migrate on the surface. As shown in Fig. 3(e), we therefore propose a
140 combination of laser desorption (red arrows) and diffusion (green arrows) to explain
141 the observed abnormal width extension in sample B. When referring to the issue of
142 surface diffusion, it is worth mentioning that the diffusion barrier along the [-110]

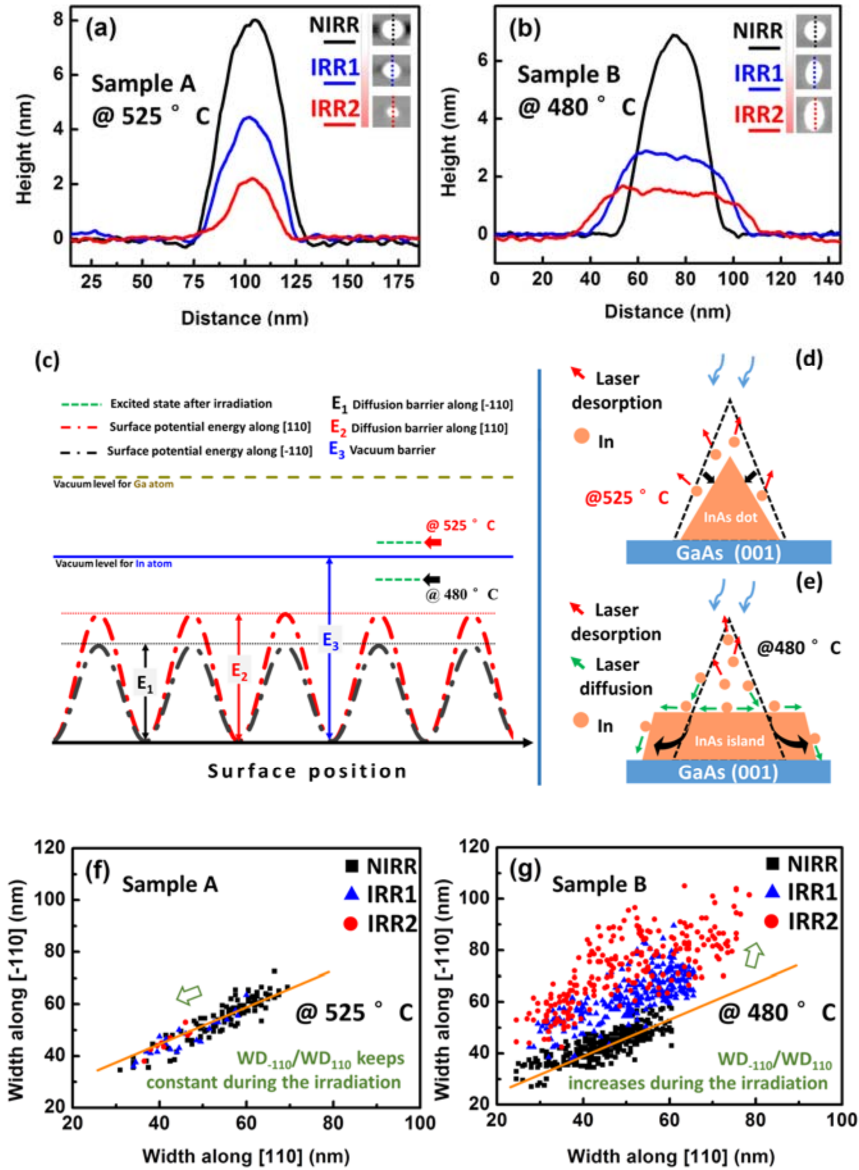

FIG. 3. (a,b) Section profiles of three typical InAs islands selected from the NIRR, IRR1, and IRR2 of (a) sample A and (b) sample B. (c) Possible excited state levels (after irradiation) for In atoms at 525 °C and 480 °C, and (d,e) the corresponding reactions of indium atoms to irradiation at (d) 525 °C and (e) 480 °C. (f,g) Relationships between the widths along the [-110] and [110] directions of the InAs islands in the NIRR, IRR1, and IRR2 of (f) sample A and (g) sample B.

143

144 direction is smaller than that along the [110]direction for In/GaAs[24,25] which usually
145 forms non-symmetrical surface morphology. Therefore, we measured the widths along
146 the [-110] (WD_{-110}) and [110] (WD_{110}) directions for all of the InAs islands shown in

147 Figs. 2(a–c), and the results are presented in Fig. 3(g). It can be clearly seen that the
148 InAs islands were elongated along the [-110] direction with an increasing WD_{-110}/WD_{110}
149 ratio after irradiation. For comparison, Fig. 3(f) shows the corresponding data
150 for sample A, in which all of the InAs QDs maintained a consistent WD_{-110}/WD_{110} ratio
151 during irradiation. In addition, the only remaining point to be clarified is why the
152 surface shown in Fig. 2(d) is so rough. It is well known that the InAs QDs grow on
153 wetting layers that are rich in indium. When these indium atoms are evaporated, the
154 original surface atomic layer will randomly crack into small fragments. When the
155 substrate temperature is not sufficiently high to provide enough surface diffusion, these
156 fragments would be unable to coalesce back in time. To test this hypothesis, we closely
157 examined three enlargements of yellow dashed squares (denoted 1–3) in Figs. 2 (a–c)
158 and clearly observed an evolution from "atomic step flow" to "atomic fragments" on
159 the background surface (as indicated at the bottom of the graphic). In contrast, the
160 background surface of sample A remained almost unchanged during LIR, which was
161 ascribed to the more efficient coalescencing (yellow dashed circles in Fig. 1(d)) at
162 higher temperature of 525 °C.

163 Taken together, the results from sample A indicate that the surface shown in Fig.
164 1(d) should has a very low concentration of defects. To thoroughly evaluate the surface
165 quality, we prepared sample C by depositing 1.8 ML of InAs at 525 °C to fully form
166 the QDs, subjected it to in situ LIR, and finally capped it with another 1.8 ML of InAs.
167 AFM and photoluminescence measurements were then conducted. The AFM
168 morphologies of the IRRC and NIRR of sample C are presented in Figs. 4(a) and (b).
169 For comparison, sample D with only a single layer of 1.8 ML InAs deposited on the
170 GaAs substrate was also prepared and the AFM results are presented in Fig. 4(c). The
171 IRRC of sample C exhibited almost the same QD morphology as sample D that means
172 the LIR cleanly lift off the first 1.8 ML InAs QD layer. While for the NIRR (Fig. 4(b)),
173 where the actual total deposition amount is 3.6 ML, both the QD density and size
174 became much larger even creating some huge InAs islands (red arrows). Furthermore,
175 the photoluminescence spectrum (Fig. 4(d)) revealed that the optical quality of the InAs
176 QDs in the IRRC was also as excellent as that of sample D, without any degradation.

177 Therefore, in situ LIR is proven to be a promising technique for the fabrication of
178 damage-resistant QDs.

179 Finally, considering that the growth temperature may also affect the wetting and
180 strain and thus afford QDs with different physicochemical properties, in order to figure
181 out whether the growth temperature also played an important role for the morphological
182 differences between sample A and B which are respectively grown at different
183 temperature. It would make more sense to comparing the dots grown at the same
184 temperature and then change the temperature before irradiation, so we prepared a final
185 sample (sample E) in which the QDs were first grown at 480 °C and then irradiated at
186 525 °C. As presented in Fig. 4(e), the evolution of the QD morphology with increasing
187 irradiation intensity behaved the same as sample A. It reflects "in situ lift-off of InAs"
188 predominantly depends on the irradiation temperature and intensity, in other words, the
189 LIR should be applicable to lift off any InAs QD regardless of its exact preparation
190 method and morphology.

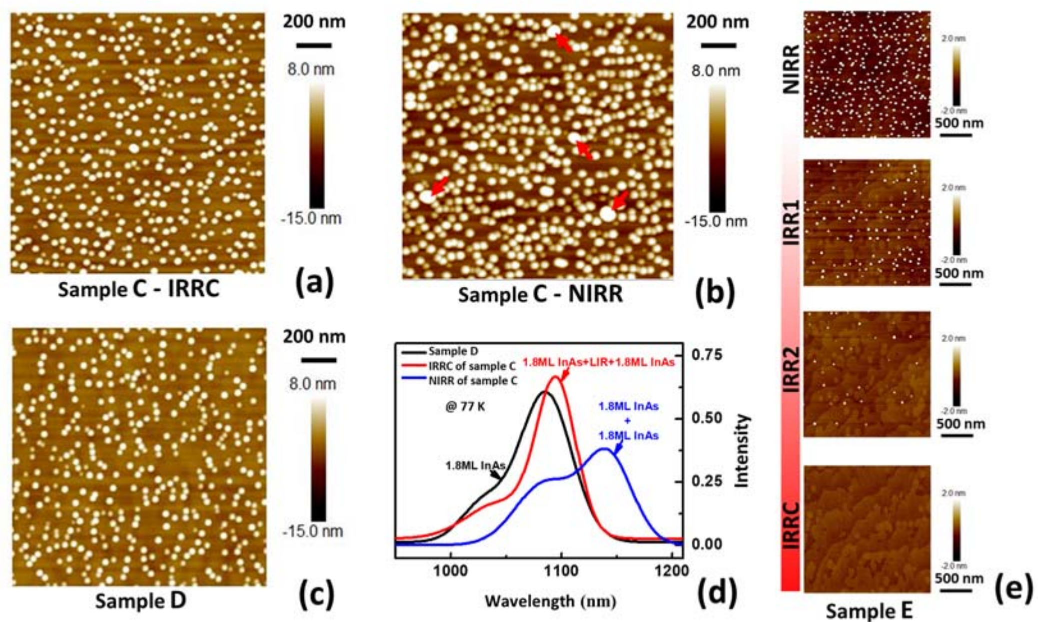

FIG. 4. (a–c) AFM morphology results of the InAs QDs in the (a) IRRC of sample C and (b) NIRR of sample C and (c) sample D, and (d) their corresponding photoluminescence spectra. (e) Evolution of the QD morphology with increasing irradiation intensity for sample E, where the QDs were grown at 480 °C and then irradiated at 525 °C.

191

192

In summary, we have investigated the in situ LIR of InAs QDs grown on a GaAs substrate by MBE. For the sample irradiated at the lower temperature (480 °C), the irradiation of the InAs QDs was found to be governed by a combination of laser-induced desorption and diffusion of indium; while for the sample irradiated at the higher temperature (525 °C), the irradiation process was dominated by laser desorption only. At both temperatures, LIR was found to induce complete lift off of the InAs QDs from the substrate. Especially for the case of 525 °C, the photoluminescence spectroscopy demonstrated that QDs subsequently grown on the irradiated surface after the LIR have exhibited the same optical quality as the common SK growth mode on an as-prepared GaAs surface. Therefore, we have developed a defect-free technology for QD fabrication by using in situ pulsed laser irradiation to lift off InAs QDs from the GaAs surface and this technology is compatible with the common epitaxy equipment with avoiding pollution and oxidation as well. In future work, we expect to facilely develop this method for the patterned lift-off of QDs by upgrading the mono-beam irradiation to multi-beam interference irradiation.

The research was supported by the National Natural Science Foundation of China (NSFC, Grant No. 11504251), the Priority Academic Program Development of Jiangsu Higher Education Institutions (PAPD), the International Cooperation Project (Grant No. 2014DFG12600) by MOST, and the Natural Science Research Project of Jiangsu Higher Education (Grant No. 12KJA140001).

[1] K. A. Fischer, L. Hanschke, J. Wierzbowski, T. Simmet, C. Dory, J. J. Finley, J. Vučković, and K. Müller, Nature Physics **13**, 649 (2017).

[2] B. S. Mashford, M. Stevenson, Z. Popovic, C. Hamilton, Z. Zhou, C. Breen, J. Steckel, V. Bulovic, M. Bawendi, S. Coe-Sullivan, and P. T. Kazlas, Nature Photonics **7**, 407 (2013).

[3] M. Davanco, J. Liu, L. Sapienza, C.-Z. Zhang, J. Vinícius De Miranda Cardoso, V. Verma, R. Mirin, S. W. Nam, L. Liu, and K. Srinivasan, Nature Communications **8**, 889 (2017).

221 [4] B. H. Kim, M. S. Onses, J. B. Lim, S. Nam, N. Oh, H. Kim, K. J. Yu, J. W. Lee, J.-H. Kim, S.-K.
222 Kang, C. H. Lee, J. Lee, J. H. Shin, N. H. Kim, C. Leal, M. Shim, and J. A. Rogers, Nano Letters
223 **15**, 969 (2015).
224 [5] D. Pan, E. Towe, and S. Kennerly, Applied Physics Letters **73**, 1937 (1998).
225 [6] J. Wu, Q. Jiang, S. Chen, M. Tang, Y. I. Mazur, Y. Maidaniuk, M. Benamara, M. P. Semtsiv, W. T.
226 Masselink, K. A. Sablon, G. J. Salamo, and H. Liu, ACS Photonics **3**, 749 (2016).
227 [7] J. Y. Yan, Q. Gong, C. Z. Kang, H. X. Xu, C. F. Cao, Y. Y. Li, S. M. Wang, and H. L. Wang, Journal
228 of Crystal Growth **425**, 373 (2015).
229 [8] B. Lingnau, K. Lüdge, B. Herzog, M. Kolarczik, Y. Kaptan, U. Woggon, and N. Owschimikow,
230 Physical Review B **94**, 014305 (2016).
231 [9] J. P. Lee, E. Murray, A. J. Bennett, D. J. P. Ellis, C. Dangel, I. Farrer, P. Spencer, D. A. Ritchie, and
232 A. J. Shields, Applied Physics Letters **110**, 071102 (2017).
233 [10] S. Suraprapapich, S. Thainoi, S. Kanjanachuchai, and S. Panyakeow, Solar Energy Materials and
234 Solar Cells **90**, 2968 (2006).
235 [11] C. E. Dimas, H. S. Djie, and B. S. Ooi, Journal of Crystal Growth **288**, 153 (2006).
236 [12] C. Y. Ngo, S. F. Yoon, W. K. Loke, Q. Cao, D. R. Lim, V. Wong, Y. K. Sim, and S. J. Chua, Applied
237 Physics Letters **94**, 143108 (2009).
238 [13] A. Imamoglu, D. D. Awschalom, G. Burkard, D. P. DiVincenzo, D. Loss, M. Sherwin, and A.
239 Small, Physical Review Letters **83**, 4204 (1999).
240 [14] E. Waks, K. Inoue, C. Santori, D. Fattal, J. Vuckovic, G. S. Solomon, and Y. Yamamoto, Nature
241 **420**, 762 (2002).
242 [15] T. F. Watson, S. G. J. Philips, E. Kawakami, D. R. Ward, P. Scarlino, M. Veldhorst, D. E. Savage,

243 M. G. Lagally, M. Friesen, S. N. Coppersmith, M. A. Eriksson, and L. M. K. Vandersypen, Nature
244 **555**, 633 (2018).
245 [16] Y. Sugimoto, N. Ikeda, N. Carlsson, K. Asakawa, N. Kawai, and K. Inoue, Journal of Applied
246 Physics **91**, 922 (2002).
247 [17] H. Z. Song, T. Usuki, T. Ohshima, Y. Sakuma, M. Kawabe, Y. Okada, K. Takemoto, T. Miyazawa,
248 S. Hirose, Y. Nakata, M. Takatsu, and N. Yokoyama, Nanoscale Research Letters **1**, 160 (2006).
249 [18] J. Tersoff, C. Teichert, and M. G. Lagally, Physical Review Letters **76**, 1675 (1996).
250 [19] V. Holý, G. Springholz, M. Pinczolits, and G. Bauer, Physical Review Letters **83**, 356 (1999).
251 [20] S. Kiravittaya, A. Rastelli, and O. G. Schmidt, Applied Physics Letters **87**, 243112 (2005).
252 [21] L. Goldstein, F. Glas, J. Y. Marzin, M. N. Charasse, and G. Le Roux, Applied Physics Letters **47**,
253 1099 (1985).
254 [22] N. N. Ledentsov, V. A. Shchukin, M. Grundmann, N. Kirstaedter, J. Böhrer, O. Schmidt, D.
255 Bimberg, V. M. Ustinov, A. Yu. Egorov, A. E. Zhukov, P. S. Kop'ev, S. V. Zaitsev, N. Yu. Gordeev,
256 Zh. I. Alferov, A. I. Borovkov, A. O. Kosogov, S. S. Ruvimov, P. Werner, U. Gösele, and J.
257 Heydenreich, Physical Review B **54**, 8743 (1996).
258 [23] M. Strassburg, V. Kutzer, U. W. Pohl, A. Hoffmann, I. Broser, N. N. Ledentsov, D. Bimberg, A.
259 Rosenauer, U. Fischer, D. Gerthsen, I. L. Krestnikov, M. V. Maximov, P. S. Kop'ev, and Zh. I.
260 Alferov, Applied Physics Letters **72**, 942 (1998).
261 [24] M. K. Yakes, L. Yang, A. S. Bracker, T. M. Sweeney, P. G. Brereton, M. Kim, C. S. Kim, P. M.
262 Vora, D. Park, S. G. Carter, and D. Gammon, Nano Letters **13**, 4870 (2013).
263 [25] M. Rosini, M. C. Righi, P. Kratzer, and R. Magri, Physical Review B **79**, 075302 (2009).